

<https://doi.org/10.22226/2410-3535-2023-2-153-157>

Thermoelectric properties of $\text{CuO-LiCoO}_2\text{-La}_{0.7}\text{Sr}_{0.3}\text{MnO}_3$ composition materials

Yu. V. Kabirov¹, M. V. Belokobylsky¹, V. R. Popov¹, A. O. Letovaltsev¹, N. V. Prutsakova^{†,2},
A. L. Nikolaev², E. V. Chebanova²

[†]shpilevay@mail.ru

¹Southern Federal University, Rostov-on-Don, 344090, Russia

²Don State Technical University, Rostov-on-Don, 344000, Russia

For the widespread use of thermoelectric materials, it is necessary to reduce their cost, simplify the technology and increase the thermoelectric figure of merit, which is highly dependent on the Seebeck coefficient. Therefore, one of the promising directions is the search for composites for effective thermoelectric converters. In our article, three-component composites consisting of a conductive component of $\text{La}_{0.7}\text{Sr}_{0.3}\text{MnO}_3$ (LSMO), and dielectric components: a mixture of CuO oxides and lithium cobaltite LiCoO_2 have been prepared and experimentally investigated as such materials. The phase composition of the obtained samples was studied by X-ray diffraction, electron and optical microscopy. The thermoelectric properties of composite materials have been studied in the field of low temperatures from 30 to 250°C. The best results for Seebeck coefficient 550 $\mu\text{V/K}$ and power factor 0.108 $\mu\text{W}/(\text{K}^2 \cdot \text{m})$ are shown by experimentally selected compositions containing about 25% by weight LSMO, 40% CuO, 30% LiCoO_2 , 5% GeO_2 . However, the largest value of the power factor 1.859 $\mu\text{W}/(\text{K}^2 \cdot \text{m})$ was achieved for the sample composition 77% LSMO, 20% CuO, 3% GeO_2 with Seebeck 310 $\mu\text{V/K}$. It should be noted that such three-phase samples have a “p”-type of conductivity. The presence of glass-forming germanium (3–5%) oxide gives samples great mechanical stability.

Keywords: composite, thermoelectric properties, copper oxides, lithium cobaltite, manganite.

1. Introduction

The development of new low-cost thermoelectric materials with high energy conversion efficiency is of great interest both from a scientific and practical point of view [1–20].

One of the reasons limiting the wide use of thermoelectric energy converters is their low thermoelectric figure of merit and power factor [13]. As is known, the efficiency Z of converting heat into electric energy is determined by the relation [2]:

$$Z = \frac{S^2 \sigma}{\lambda}, \quad (1)$$

where S is the Seebeck coefficient, $S = \Delta U / \Delta T$, $\Delta T = T_2 - T_1$ (T_1 and T_2 are the temperatures of the hot and cold edges of the sample, respectively), σ is the electrical conductivity, λ is the thermal conductivity. The Ioffe parameter ZT is also used to estimate figure of merit, where T is the average temperature equal to:

$$T = (T_1 + T_2) / 2 \quad (2)$$

The thermoelectric power factor P was estimated by the expression:

$$P = S^2 \sigma \quad (3)$$

It is obvious that materials for efficient thermoelectric energy converters must have a high Seebeck coefficient,

good conductivity and low thermal conductivity. [12,15]. According to [3], the search for composites is a promising direction due to the combination of high conductivity values and a Seebeck coefficient with low thermal conductivity values of such multiphase materials. Therefore, it is hoped that the desired high figure of merit values of the thermal energy conversion can be obtained in composite materials. In turn, composites based on copper oxides and compounds are promising systems due to the high value of the Seebeck coefficient is about 500 $\mu\text{V/K}$ [4–7,17–19]. The figure of merit of such systems can be increased by increasing the electrical conductivity by introducing conductive fillers into them. The researchers pay special attention to compositions with copper oxides — Cu_2O and CuO , with a band gap of 2.2 and 1.2 eV, respectively. Copper oxide CuO is more stable, has a low price, is non-toxic, and is a p-type semiconductor having monoclinic symmetry. With a high value of the Seebeck coefficient, it has a low figure of merit due to its high thermal conductivity. Thus, in work [4], thin-layer composites of the composition CuO and single-wall carbon nanotubes (SWCNTs) low concentration were prepared. The use of carbon nanotubes allowed to increase the Seebeck factor and power factor to 882 $\mu\text{V/K}$ and 2500 $\mu\text{W} \cdot \text{m}^{-1} \cdot \text{K}^{-2}$, respectively, at 673 K. However, for such composites at low temperatures up to 500 K, the situation changes dramatically. The Seebeck factor and power factor have values of 300 $\mu\text{V/K}$ and less than 100 $\mu\text{W} \cdot \text{m}^{-1} \cdot \text{K}^{-2}$. Given the astronomical price

of SWCNT today, such compositions are unlikely to become widespread in thermoelectric generators. In [5,6] studied the electrical properties of nanocomposites based on the oxide phases of CuO and Cu₂O, where carbon nanofibers were used as a filler. The achieved values of the Seebeck coefficient amounted to values, about 800–1000 $\mu\text{V}/\text{K}$, at power factor of order 500 $\mu\text{W}\cdot\text{m}^{-1}\cdot\text{K}^{-2}$. However, these composites have such values at a low temperature below 300 K. Under normal conditions, the S values are reduced to 500 $\mu\text{V}/\text{K}$.

In turn, [17] studied the thermoelectric properties of CuO doped with alkali metal ions (Li, Na, K), while the power factor was 160 $\mu\text{W}\cdot\text{m}^{-1}\cdot\text{K}^{-2}$, and the Seebeck coefficient is of the order of 500 $\mu\text{V}/\text{K}$. In article [9], in the composition of K_{0.2}Cu_{1.8}S at a temperature above 300°C, there is a significant increase the coefficient Seebeck to 4 mV/K.

In the article [7] examined the electrical resistance and thermoelectric properties of nanocomposites obtained by introducing copper particles into an amorphous carbon matrix. Study of thermoelectric properties of superionic alloys Ag_xCu_{2-x}Se [8] and K_xCu_{2-x}S [9] showed the presence of good thermoelectric figure of merit only in the field of high temperatures. As noted in [10], lithium cobaltites with different replacement of lithium ions with transition metal ions have a special perspective in the field of thermoelectricity. Terekhov et al [11] obtained sodium cobaltites by solid phase method, investigated their electrical and functional properties. In the article [14] studied the concentration and temperature dependencies of thermoelectric properties of composites with metal inclusions of Co nanoparticles in an amorphous dielectric matrix Al₂O_n. Mulla and Rabinal [18] studied the thermoelectric properties of composites CuO/Cu_xS, and achieved significant values of the thermoelectric power factor, of the order of 10 $\mu\text{W}\cdot\text{m}^{-1}\cdot\text{K}^{-2}$, with a Seebeck factor of 500 $\mu\text{V}/\text{K}$. However, obviously such compositions do not exhibit temperature stability at temperatures above 100°C. The paper [19] demonstrates the prospects of integrating ZnO and CuO nanowire into a series of thermocouples to create new efficient thermoelectric devices. In [20], an affordable technology for the manufacture of flexible thermoelectric sensors based on copper oxide Cu₂O and graphite-polymer paste was presented.

2. Formulation of the problem

The ideology of our experiment is related to the possibility of increasing the power factor of compositions containing dielectric components, such as copper oxide CuO with a narrow band gap, as well as lithium cobaltite LiCoO₂ and a third component with good conductivity La_{0.7}Sr_{0.3}MnO₃ (LSMO) [21]. The thermoelectric properties of these composite materials have been studied in the temperature field of 30–250°C. The current task was the need to achieve the maximum value of the Seebeck coefficient S and the power factor, varying the component ratios.

3. Experiment

The starting materials were first homogenized and then pressed under pressure 300 MPa, then annealed at 950°C for three hours. The percentage of the three components was

changed in increments of 5%, with the number of possible variants exceeding 300. However, in view of the fact that compositions with a large content of conductive or dielectric components cannot have a high Seebeck coefficient and maximum power, respectively, we have narrowed the range of options, limiting ourselves to the consideration of about 100 composites. In all cases, a small addition of germanium oxide GeO₂ was used to improve the ceramic properties. [22]. It should be noted that such three-phase composites have a “p”-type of conductivity. The samples are disks with a diameter of 10–12 mm and a thickness of 3–5 mm. The density of the samples is in the range from 2.5 g/cm³ and up to 6.2 g/cm³. Porosity of samples of the order of 10%.

Figure 1 shows the scheme of the experiment for measuring the Seebeck coefficient.

Seebeck ratio measurement error did not exceed 4–5%. The prepared ceramics before and after annealing were tested on a D8 Brooker Advance X-ray diffractometer by CuK_α radiation with a wavelength of 1.5406 Å. Results were processed by Rietveld full-profile analysis.

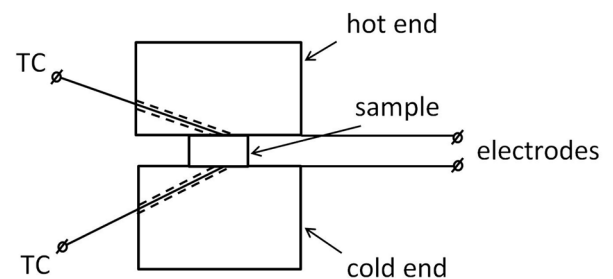


Fig. 1. Scheme of the experiment, TC — thermocouple.

4. Results and discussion

X-ray diffraction results indicate that after the annealing, copper oxide Cu₂O (space group *Pn3m*, $a=4.2893$ Å) almost completely changed to CuO (space group *C2/c*, cell parameters $a=4.6841$ Å, $b=3.3903$ Å, $c=5.1279$ Å). The remaining components are preserved with some parameter changes. So, for LSMO (space group *R3c*) cell parameters of the initial sample $a=5.5230$ Å, $c=13.349$ Å, after annealing $a=5.5421$ Å, $c=13.361$ Å. For LiCoO₂ (space group *R3m*) cell parameters of the initial sample $a=2.826$ Å, $c=14.120$ Å, after annealing $a=2.8405$ Å, $c=14.195$ Å. Figure 2 shows the X-ray pattern of the composition sample for example: CuO — 40%, LiCoO₂ — 30%, LSMO — 25%, GeO₂ — 5% mass. after annealing.

X-ray diffraction of initial mixtures before and after annealing (Fig. 2) allows to make the following conclusions. The original Cu₂O component completely switched to CuO after annealing. For LiCoO₂ delafossite and LSMO manganite, while maintaining structure after annealing, diffraction reflections are widened, which indicates an increase in the degree of defectiveness and grinding of coherent-scattering region and increasing cell parameters. Sizing assessment of the coherent-scattering region for delafossite LiCoO₂ according to the Scherrer ratio gives the following values: before annealing 96 nm, after — 60 nm. For

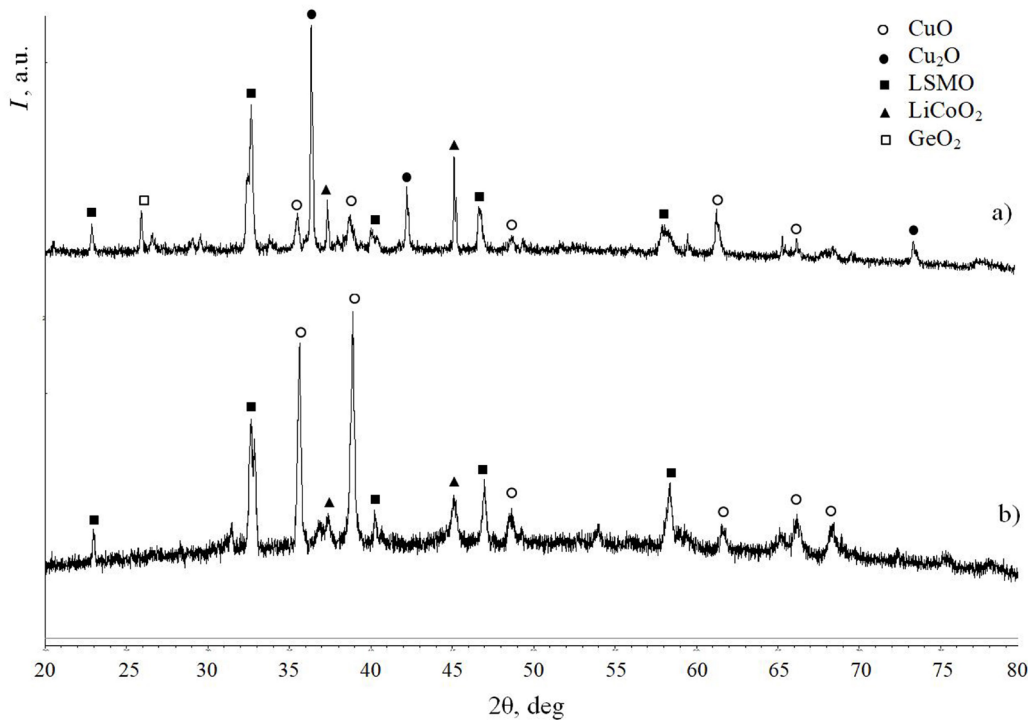


Fig. 2. X-ray diffraction pattern of the composite sample of the composition Cu_2O — 34%, CuO — 6%, LiCoO_2 — 30%, LSMO — 25%, GeO_2 — 5% before annealing (a), X-ray diffraction pattern of the composite sample of the composition CuO — 40%, LiCoO_2 — 30%, LSMO — 25%, GeO_2 — 5% after annealing (b).

LSMO manganite, coherent-scattering region sizes retained their values. It should be noted that germanium oxide after annealing leaves in the glassy amorphous phase of the GeO_2 oxide, which is expressed in an X-ray pattern by a bell-shaped background (Fig. 2).

To analyze the microstructure of the composites, transverse chips of the ceramic were examined using a Carl Zeiss EVO 40 scanning electron microscope, while the chips were not subjected to preliminary mechanical processing. To remove the surface charging effects, a metal electrically conductive layer was additionally applied using a Quorum SC7620 Mini Sputter magnetron spraying unit for 15 seconds in an argon atmosphere at a current of 18 mA. Raster images were obtained using an Everhart-Thornley SE secondary electron detector at an accelerating voltage of 20 kV, operating distances of 7–8 mm and a probe current of 20 pA. Micrographs of ceramic samples are shown in Fig. 3, where crystallites bound by a glass-forming compound are clearly visible. To control the elemental composition, an Oxford Instruments X–Max 80 X-ray microanalyzer was used.

Note that the particle sizes of manganite (dark areas) are of the order of 2–3 μm . Light crystallites, dielectric composition — copper oxide — have a large variation in size, from one to 8 μm . Gray fields are dispersed lithium cobaltite.

The results of the study of the thermoelectric properties of the composite materials showed that the sign of the charge carriers does not change and remains positive over the entire temperature range under study, and the energy of activation of the samples depends on temperature. This fact indicates that the main carriers of charge are holes, as well as in the work [6] on the study of copper oxide composites — carbon nanofibers. In the studied temperature range of 30–250°C,

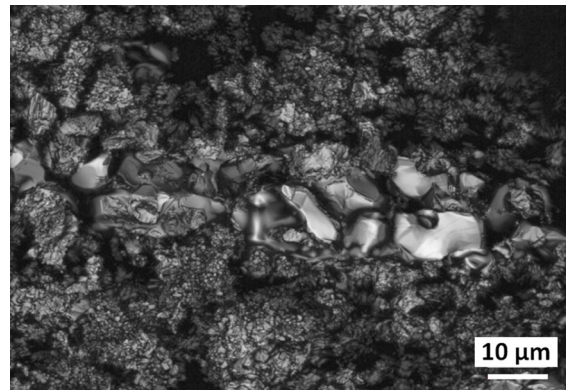


Fig. 3. SEM-image of the surface of the sample chip CuO — 40%, LiCoO_2 — 30%, LSMO — 25%, GeO_2 — 5%.

charge carrier activation energy of samples with the best values of the Seebeck coefficient (about 550 $\mu\text{V/K}$) averages 0.3 eV. For comparison, we note that pure copper oxide CuO had a Seebeck coefficient of about $\approx 630 \pm 10 \mu\text{V/K}$ [18]. The electrical resistance of composites with different components percentages varies depending on the temperature in the range from 20 to 1100 Ohm. Figure 4 shows typical conductivity versus inverse temperature relationships for some composites.

In the studied temperature range, the conductivity pattern for the CuO sample is 40%, LiCoO_2 — 30%, LSMO — 25%, GeO_2 — 5% has an almost linear appearance, which indicates the temperature-activation type of conductivity. With an increase in the content of germanium oxide to 8% by weight, a completely different behavior of conductivity is observed — almost independent of temperature. Given the complexity of the test formulation, this conduction behavior requires

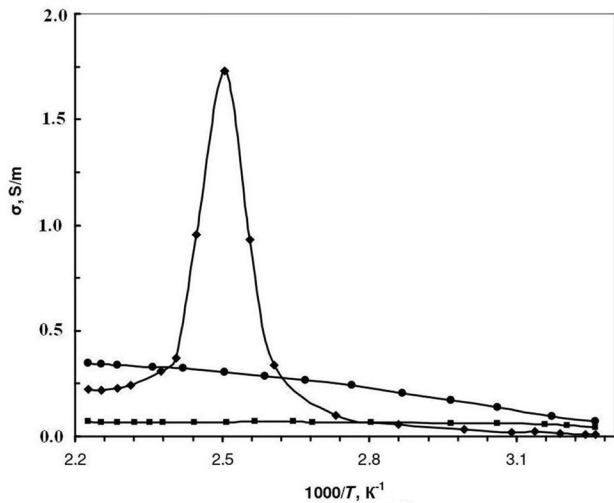


Fig. 4. Conductivity for some composites:
 • CuO — 40%, LiCoO₂ — 30%, LSMO — 25%, GeO₂ — 5%,
 ■ CuO — 32%, LiCoO₂ — 30%, LSMO — 25%, GeO₂ — 8%,
 ◆ CuO — 19%, LiCoO₂ — 30%, LSMO- 48%, GeO₂ — 3%.

further investigation. Composites with a high content of LSMO manganite (48% and above) in the region of its stretched phase transition show an increase in conductivity, which corresponds to the data of work [21].

Figure 5 shows the dependences of the Seebeck ratio and the power factor on the average temperature of hot and cold edges according to Eq. (2) for the composite composition of CuO — 40%, LiCoO₂ — 30%, LSMO — 25%, GeO₂ — 5%.

Note the strong influence of component concentration ratios on the thermoelectric properties of the obtained samples. As noted in [17], the ion radius Li⁺ (0.76 Å) is close to the radius Cu²⁺ (0.73 Å). This contributes to Cu vacancies or some replacements substitution of Cu²⁺ ions by Li⁺ with an increase in the concentration of the holes, and increased holes conductivity in composites with CuO. This fact can affect the conductivity of such composites.

Table 1 shows the results of measuring the Seebeck coefficient for composites of different compositions in the low-temperature region with a temperature difference of hot and cold edges ΔT=15 K. The average temperature of the hot and cold ends of the samples is 313 ± 2 K.

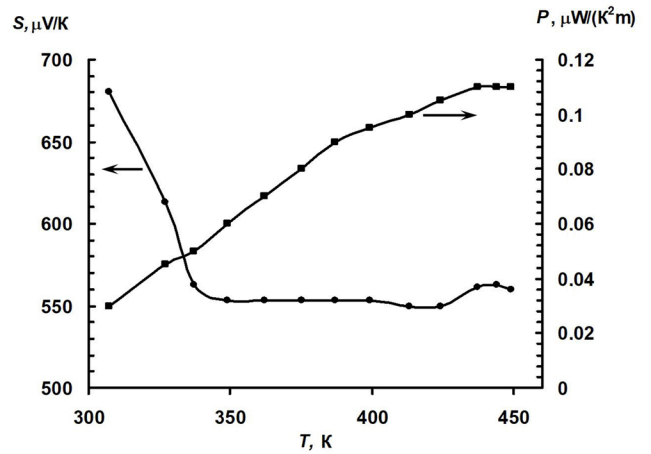


Fig. 5. The dependences of the Seebeck coefficient S and the power factor P on the average temperature T of hot and cold edges for the composite of CuO — 40%, LiCoO₂ — 30%, LSMO — 25%, GeO₂ — 5%.

As can be seen from the above results, there is a balance of ratios between components for optimal values of thermoelectric properties, the Seebeck coefficient decreases sharply with a decrease in copper oxide concentration, and a similar effect exists for compositions with a reduced content of the conductive component — lanthanum strontium manganite, LSMO. The best results for the Seebeck coefficient are given by experimentally selected formulations containing 25% by weight LSMO, 40% CuO and 30% LiCoO₂. It should be noted that for composite No. 2, in the absence of lithium cobaltite, a high power factor is observed with a decrease in the Seebeck coefficient. This result will be studied in the future. However, such compositions with a high LSMO content may be expensive due to the presence of a rare-earth lanthanum element therein.

As noted in [23], the best thermoelectric semiconductor compositions today are AgPb_mSbTe_{2+m}, (Bi, Sb)₂Te₃, but at the same time the prevalence of antimony and tellurium is very small, not to mention the toxicity of elements such as lead and antimony. For copper, the situation is completely different, this is a very common metal, and accordingly, its oxide. Given the technology of preparing semiconductor compositions, it can be argued that the ceramic compositions proposed in our

Table 1. Seebeck factor and power factor for some composites of different composition.

No.	Weight ratio of composite components				Seebeck coefficient μV/K	Power factor, μW/(K ² ·m)
1	CuO 40%	LiCoO ₂ 30%	LSMO 25%	GeO ₂ 5%	550	0.108
2	CuO 20%	0%	LSMO 77%	GeO ₂ 3%	310	1.859
3	CuO 40%	LiCoO ₂ 30%	LSMO 26%	GeO ₂ 4%	513	0.009
4	CuO 19%	LiCoO ₂ 30%	LSMO 48%	GeO ₂ 3%	195	0.01
5	CuO 20%	LiCoO ₂ 20%	LSMO 57%	GeO ₂ 3%	60	0.001
6	CuO 35%	LiCoO ₂ 35%	LSMO 27%	GeO ₂ 3%	206	0.037
7	CuO 10%	LiCoO ₂ 65%	LSMO 22%	GeO ₂ 3%	11	0.0002
8	CuO 40%	LiCoO ₂ 30%	LSMO 26%	GeO ₂ 4%	213	0.011
9	CuO 22%	LiCoO ₂ 25%	LSMO 50%	GeO ₂ 3%	90	0.00004
10	CuO 32%	LiCoO ₂ 30%	LSMO 35%	GeO ₂ 3%	333	0.011
11	CuO 30%	LiCoO ₂ 10%	LSMO 57%	GeO ₂ 3%	103	0.004
12	CuO 39%	LiCoO ₂ 30%	LSMO 27%	GeO ₂ 4%	170	0.002
13	CuO 16%	LiCoO ₂ 40%	LSMO 40%	GeO ₂ 4%	214	0.008

work have a significant technological advantage in the ease of preparation.

According to the ideology of work [2], the values of activation energy observed in our work (about 0.2–0.3 eV) make it possible at temperatures below 400°C to reduce the effects associated with the presence of carriers of the second sign. It should also be noted that the optimal Z values given for semiconductors at certain ratios of Seebeck coefficient and conductivity in works [2, 24] in the case of oxide composite compositions cannot be used directly. This is due to a different physical mechanism of conductivity in composites compared to narrow band semiconductors [24].

According to the estimates of operation [15], it is the combination of good conductive components with semiconductor thermoelectric components that gives high values of the power factor compared to “pure” thermoelectric materials. According to the authors, for this it is necessary to create alternating structures of the conductor and the thermoelectric dielectric. This conclusion is indeed supported in our work.

Thus, the possibility of using prepared composites at low temperatures (up to 250°C) is also shown. Such composites are stable under conventional conditions as they are oxide materials. It is highly likely that the fabricated oxide materials can be operable at higher temperatures as well, which requires further study. Note that such compositions, apparently, can be used in radioisotope energy sources, since the radiation resistance of ceramic materials is very high — it can reach 10^{20} Gy [25].

Acknowledgments. This work was supported partially by the Russian Science Foundation (RSF) through grant No. 19-19-00444, <https://rscf.ru/project/19-19-00444/>.

5. Conclusions

Composite materials of the composition: CuO, LiCoO₂, LSMO with different ratios of components were annealed. Their thermoelectric properties, a power factor in the temperature range from 30 to 250°C, have been studied. Promising studies of composite materials based on CuO, LiCoO₂, La_{0.7}Sr_{0.3}MnO₃ for their use in thermoelectric devices are shown. For the composition of CuO 40%, LiCoO₂ 30%, LSMO 25% and GeO₂ 5%, Seebeck coefficient values of the order of 500 μV/K were achieved with a power factor of 0.1 μW·m⁻¹·K⁻². Thus, the potential for creating thermoelectric materials based on copper oxide and cobalt compositions with a conductive component is far from being exhausted.

References

1. L.D. Ivanova. Semiconductors. 51 (7), 909 (2017). [Crossref](#)
2. A.F. Ioffe. Semiconductor thermoelements. Moscow, Leningrad, AN SSSR (1956) 104 p. (in Russian)
3. S.A. Gridnev, Yu. E. Kalinin, V.A. Makagonov. Alternative energy and ecology. 34–36, 41 (2019). (in Russian)
4. N. Salah, N. Baghdadia, A. Alshahria, A. Saeeda, A.R. Ansaria, A. Memica, K. Koumotoa. Journal of the European Ceramic Society. 39 (11), 3307 (2019). [Crossref](#)
5. Yu. E. Kalinin, V.A. Makagonov, Yu. V. Panin, A. S. Shuvaev. Bulletin of VSTU. 11, 57 (2012). (in Russian)
6. Yu. E. Kalinin, V.A. Makagonov, Yu. V. Panin, Yu. A. Shchetinin. International Scientific Journal Alternative Energy and Ecology. 8 (130). 84 (2013). (in Russian)
7. V.A. Makagonov, A.S. Krasnova, L.I. Yanchenko, I.M. Tregubov, M.A. Kashirin. Bulletin of the Voronezh State Technical University. 13 (6), 104 (2017). (in Russian)
8. M.K. Balapanov, R.K. Ishembetov, K.A. Kuterbekov, M.M. Kubenova, V.N. Danilenko, K.S. Nazarov, R.A. Yakshibaev. Letters on Materials. 6 (4), 360 (2016). (in Russian) [Crossref](#)
9. M.K. Balapanov, R.K. Ishembetov, K.A. Kuterbekov, A.K. Baisheva, R.S. Palymbetov, S. Sakhabaeva, M.M. Kubenova, R.A. Yakshibaev. Letters on Materials. 10 (4), 439 (2020). (in Russian) [Crossref](#)
10. G.G. Gromov. Components & technologies. 8, 108 (2014). (in Russian)
11. D.Yu. Terekhov, A.A. Sherchenkov, I.A. Voloshchuk, D.V. Pepelyaev, M.Yu. Stern, P.I. Lazarenko, A.O. Yakubov, A.V. Babich. Nanotechnologies in Russia. 16 (3), 429 (2021). (in Russian) [Crossref](#)
12. A.V. Dmitriev, I.P. Zvyagin. Phys.-Usp. 53, 789 (2010). [Crossref](#)
13. A.V. Simkin, A.V. Biryukov, N.I. Repnikov, V.V. Khovailo. Bulletin of the ChSU. 7, 362 (2015). (in Russian)
14. V.A. Belousov, A.B. Granovsky, Yu. E. Kalinin, A.V. Sitnikov. Phys. Solid State. 49 (10), 1848 (2007). [Crossref](#)
15. D.N. Trunov, E.S. Klementyev. Journal of Surface Investigation: X-ray, Synchrotron and Neutron Techniques. 12, 57 (2013). (in Russian) [Crossref](#)
16. B. Poudel, Q. Hao, Y. Ma, X.Y. Lan, A. Minnich, B. Yu, X. Yan, D.Z. Wang, A. Muto, D. Vashaee, X.Y. Chen, J.M. Liu, M.S. Dresselhaus, G. Chen, Z.F. Ren. Science. 320 (5876), 634 (2008). [Crossref](#)
17. N. Yoshida, T. Naito, H. Fujishiro. Japanese Journal of Applied Physics. 52, 031102 (2013). [Crossref](#)
18. R. Mulla, M.K. Rabinal. Materials for Renewable and Sustainable Energy. 10, 3 (2021). [Crossref](#)
19. D. Zappa, S. Dalola, G. Faglia, E. Comini, M. F. C. Soldano, V. Ferrari, G. Sberveglieri. Beilstein J. Nanotechnol. 5, 927 (2014). [Crossref](#)
20. A. Virgil, K. Bethkea, K. Rademann. Phys. Chem. Chem. Phys. 18, 10700 (2016). [Crossref](#)
21. A.A. Urushibara, Y. Moritomo, T. Arima, A. Asamitsu, G. Kido, Y. Tokura. Phys. Rev. B. 51, 14103 (1995). [Crossref](#)
22. A. Fel'ts. Amorphous and glassy inorganic solids. Moscow, Mir (1986) 558 p. (in Russian)
23. P. Vaqueiro, A.V. Powell. J. Mater. Chem. 20, 9577 (2010). [Crossref](#)
24. C. Wood. Rep. Prog. Phys. 51, 459 (1988). [Crossref](#)
25. N.S. Zefirov et al. Chemical encyclopedia. T.4. Moscow, Bolshaya Rossiiskaya Enzik. (1995) 641 p. (in Russian)